

Numerical Heat Transfer, Part B: Fundamentals



ISSN: 1040-7790 (Print) 1521-0626 (Online) Journal homepage: http://www.tandfonline.com/loi/unhb20

THE NORMALIZED WEIGHTING FACTOR METHOD: A NOVEL TECHNIQUE FOR ACCELERATING THE CONVERGENCE OF HIGH-RESOLUTION CONVECTIVE SCHEMES

M. S. Darwish & F. Moukalled

To cite this article: M. S. Darwish & F. Moukalled (1996) THE NORMALIZED WEIGHTING FACTOR METHOD: A NOVEL TECHNIQUE FOR ACCELERATING THE CONVERGENCE OF HIGH-RESOLUTION CONVECTIVE SCHEMES, Numerical Heat Transfer, Part B: Fundamentals, 30:2, 217-237, DOI: 10.1080/10407799608915080

To link to this article: http://dx.doi.org/10.1080/10407799608915080



Full Terms & Conditions of access and use can be found at http://www.tandfonline.com/action/journalInformation?journalCode=unhb20

THE NORMALIZED WEIGHTING FACTOR METHOD: A NOVEL TECHNIQUE FOR ACCELERATING THE CONVERGENCE OF HIGH-RESOLUTION CONVECTIVE SCHEMES

M. S. Darwish and F. Moukalled

American University of Beirut, Department of Mechanical Engineering, P.O. Box 11-0236, Beirut, Lebanon

This article deals with the development of a new method for accelerating the solution of flow problems discretized using high-resolution convective schemes. The technique is based on the normalized variable and space formulation (NVSF) methodology and is denoted here by the normalized weighting-factor (NWF) method. In contrast with the well-known deferred-correction (DC) procedure, the NWF method is fully implicit and is derived by directly replacing the control-volume face values by their functional relationships in the discretized equation. The direct substitution is performed by the introduction of a variable, NWF, that accounts for the multiplicity of interpolation profiles in HR schemes. The new method is compared with the widely used DC procedure and is shown to be, on average, four times faster.

INTRODUCTION

In many areas of computational fluid dynamics (CFD), especially convective heat and mass transfer, the upwind-based class of schemes (hybrid [1], power-law [2], etc.), denoted here by low-order (LO) schemes, have been and are still widely used despite their well-known deficiency of being highly diffusive [3]. The popularity of these methods for steady-state computations stems from a combination of algorithmic simplicity, fast convergence (implicit terms), and plausible-looking results (free from oscillations and over- or undershoots). By contrast, a limited number of problems have been solved using higher-order (HO) schemes, which suffer convergence difficulties (second-order central) [4] and oscillatory behaviors (second-order upwind, QUICK scheme) [5].

Over the last decade, researchers have tried to eliminate the shortcomings of HO schemes. Their work has led to the development of what is known as the high-resolution (HR) schemes [6, 7]. High-resolution schemes denote the class of composite HO schemes that are bounded and have relatively low numerical diffusion. The different streams followed in the design of these schemes have been unified within the context of the normalized variable and space formulation

Received 10 November 1995; accepted 23 February 1996.

The financial support provided by the University Research Board of the American University of Beirut through grants No. 48120 and 48122 is gratefully acknowledged.

Address correspondence to Dr. F. Moukalled, Department of Mechanical Engineering, American University of Beirut, P.O. Box 11-0236, Beirut, Lebanon.

NOMENCLATURE								
Α	coefficients of the discretized equation	Superscrip	ots					
В	source term in the discretized equation	C D	convection contribution diffusion contribution					
С	convective flux coefficient at control-volume face	LO	low-order scheme formulation refers to normalized variables					
f() J	functional relationship total scalar flux across cell face	Subscripts						
k m	intercept in NVD slope in NVD	С	central grid point					
QRE	source term residual error	D dc	downstream grid point deferred correction					
S	surface area of control-volume face		refers to neighbors of the P grid					
u, v	velocity components in the x and y directions	e, w, n, s f	refers to control-volume faces refers to control-volume face					
r	diffusion coefficient	NB	refers to neighbors					
ϕ	density general dependent variable	P U	main grid point upstream grid point					

(NVSF) methodology [8], and a large number of total variational diminishing flux-limiter (TVD) [9] schemes have already been reformulated using the NVSF notation [8]. The numerical implementation of these schemes has been simplified through the use of the deferred-correction (DC) procedure [10], thus preserving codes based on LO schemes by the addition of a source term that accounts for the difference in interpolated values between the HR scheme and the LO scheme, at the price of a reduced convergence rate and an increased computational cost. These problems meant that the highly diffusive LO schemes remained popular in spite of their more and more documented inadequacies [11].

A number of attempts have been made to alleviate the above-mentioned problems, such as the downwind weighting-factor (DWF) method of Leonard [12] and the variable curvature-factor (VCF) procedure of Gaskell and Lau [13]. Neither technique, however, provides an efficient method that can be applied to the class of HR schemes, which means that the DC procedure has remained the preferred method for implementing HR schemes.

In this article, the high-computational-cost problem of HR schemes is addressed and a new technique for accelerating the convergence rate of these schemes is presented. The new approach, denoted here the normalized weighting-factor (NWF) method, may be used with any scheme that can be formulated using the framework of the NVSF methodology (basically, all TVD-based schemes plus a number of third-order HR schemes). The new NWF method is compared, in terms of computer time and number of iterations needed to obtain a converged solution, with the widely used DC procedure. This is done by solving for two test problems employing a number of HO and HR schemes (QUICK [5], SOU [4], SMART [13], MINMOD [14], OSHER [15], MUSCL [16], and FROMM [17]). The results obtained show the superiority of the new NWF method over the DC procedure.

In what follows, the mathematics of the approach are presented. This is achieved by briefly describing the discretization procedure of the governing conservation equation and the NVSF methodology. Then, the DC, DWF, and VCF techniques are reviewed and their deficiencies pointed out. Finally, the new NWF method is detailed and used along with the DC approach to solve the two test problems.

NUMERICAL DISCRETIZATION OF THE TRANSPORT EQUATION

The transport equation governing two-dimensional incompressible steady flows may be expressed in the following form:

$$\tilde{\nabla} \cdot (\rho \tilde{\mathbf{u}} \phi) = \tilde{\nabla} \cdot (\Gamma \tilde{\nabla} \phi) + Q \tag{1}$$

where ϕ is any dependent variable, \mathbf{u} is the velocity vector, and ρ , Γ , and Q are the density, diffusivity, and source terms, respectively. Integrating the above equation over the control volume shown in Figure 1 and applying the divergence theorem, the following discretized equation is obtained:

$$J_{e} + J_{w} + J_{n} + J_{s} = B \tag{2}$$

where J_f represents the total flux of ϕ across cell face f (f = e, w, n, or s), and B is the volume integral of the source term Q. Each of the surface fluxes J_f contains a convective contribution, J_f^C , and a diffusive contribution, J_f^D , hence

$$J_{\rm f} = J_{\rm f}^C + J_{\rm f}^D \tag{3}$$

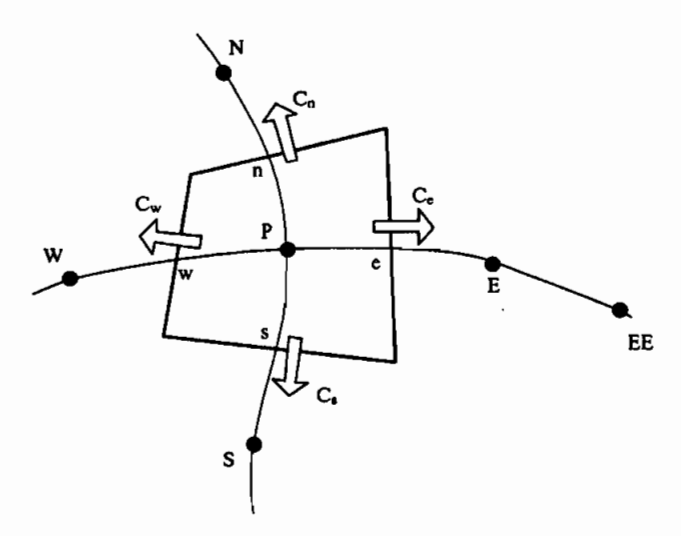


Figure 1. Control volume.

For purely convective scalar flows (such as those considered in this work), the diffusion flux, J_f^D , is zero, while the convective flux is given by

$$J_f^C = (\rho \mathbf{u} \cdot \mathbf{S})_f \phi_f = C_f \rho_f \tag{4}$$

where S_f is the surface of cell face f, and C_f is the convective flux coefficient at cell face f. As can be seen from Eq. (4), the accuracy of the control-volume solution for the convective scalar flux depends on the proper estimation of the face value of ϕ_f as a function of the neighboring ϕ node values. Using some assumed interpolation profile, ϕ_f can be explicitly formulated in terms of its node values by a functional relationship of the form

$$\phi_{\rm f} = f(\phi_{\rm NB}, C_{\rm f}) \tag{5}$$

where ϕ_{NB} denotes the neighboring ϕ node values (ϕ_E , ϕ_W , ϕ_N , ϕ_S , ϕ_P , ϕ_{EE} , ϕ_{WW} , ϕ_{NN} , ϕ_{SS} , etc.). Substituting Eq. (4) into Eq. (2) for each cell face yields

$$C_e \phi_e + C_w \phi_w + C_n \phi_n + C_s \phi_s = B \tag{6}$$

By replacing the face values by their functional relationships [Eq. (5)], Eq. (6) is transformed after some algebraic manipulations into the following discretized equation:

$$A_{P}\phi_{P} = \sum_{NB=E,W,N,S,...} A_{NB}\phi_{NB}B_{I}$$
 (7)

where the coefficients $A_{\rm P}$ and $A_{\rm NB}$ depend on the selected scheme and $B_{\rm P}$ is the source term.

While this direct method is appropriate for HO schemes such as the secondorder upwind scheme [4] and the QUICK scheme [5], it is not suitable for HR schemes, for which a direct substitution of the functional relationships cannot be performed because of their composite nature; i.e., multiple interpolation profiles are used with a switching criterion depending on the local flow conditions. To solve this problem, a number of approaches have been advertised, as described next.

NORMALIZED VARIABLES AND BOUNDEDNESS CRITERION

The main problem associated with HO schemes is boundedness. This deficiency has been removed through the introduction of the convection boundedness criterion (CBC) [18, 13], which has led to the development of HR schemes in the context of the NVF [6] and NVSF [8] methodologies. However, boundedness has been achieved at the expense of the convergence rate. This is so because the various techniques developed rely directly (DC method) or indirectly (DWF and VCF methods) on explicit terms. Even though the VCF method may in some cases be fully implicit, the continuous variation of its curvature factor, when explicitness exists (as explained later), slows down its convergence rate and reduces its usefulness.

In order to clarify the above statements, the DC, DWF, and VCF methods should be introduced and discussed. However, their introduction necessitates knowledge of the CBC, which is presented next along with the NVSF methodology.

Normalized Variables

Figure 2 shows the local behavior of the convected variable near a control-volume face. The node labeling refers to the upstream, central, and downstream grid points, designated by U, C, and D, located at distances ξ_U , ξ_C , and ξ_D from the origin, respectively. The values of ϕ at these nodes are designated at ϕ_U , ϕ_C , and ϕ_D , respectively. Moreover, the value of the dependent variable at the control-volume face located at a distance ξ_f from the origin is expressed by ϕ_f . Since a normalized variable and space formulation is sought, the following normalized variables are defined [8]:

$$\tilde{\phi} = \frac{\phi - \phi_{\mathrm{U}}}{\phi_{\mathrm{D}} - \phi_{\mathrm{U}}} \qquad \tilde{\xi} = \frac{\xi - \xi_{\mathrm{U}}}{\xi_{\mathrm{D}} - \xi_{\mathrm{U}}} \tag{8}$$

Using $\tilde{\phi}_f$, the functional relationships for all schemes of order 3 and less may be simplified. For example, the functional relationships of the upwind, central difference, second-order upwind, FROMM, and QUICK schemes are as given in Table 1 [8].

Convection Boundedness Criterion

Boundedness requires that the approximated finite-volume face value ϕ_f lies within the bounds of its neighboring nodes ϕ_C and ϕ_D . The violation of the boundedness is the cause of overshoots and/or undershoots in the computed results.

The CBC for implicit steady-state flow calculations, as formulated by Gaskell and Lau [13], may be stated based on the normalized variable analysis as follows. For a scheme to have the boundedness property, its functional relationship should be continuous and bounded from below by $\tilde{\phi}_{\rm f} = \tilde{\phi}_{\rm C}$ and from above by unity, should pass through the point (0,0) and (1,1) in the monotonic range $0 < \tilde{\phi}_{\rm C} < 1$,

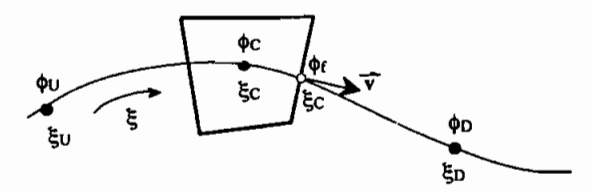


Figure 2. Local coordinate system.

Table 1. Functional relationships for higher-order schemes

	Normalized functional relationships			
Scheme	Nonuniform grid (NVSF)	Uniform grid (NVF)		
First-order upwinding	$ ilde{\phi}_{ m f} = ilde{\phi}_{ m C}$	$ ilde{\phi}_{\mathrm{f}} = ilde{\phi}_{\mathrm{C}}$		
Second-order upwinding	$egin{aligned} & ar{\phi}_{\mathrm{f}} = ar{\phi}_{\mathrm{C}} \\ & ar{\phi}_{\mathrm{f}} = rac{ar{\xi}_{\mathrm{f}}}{ar{\xi}_{\mathrm{C}}} ar{\phi}_{\mathrm{C}} \end{aligned}$	$ ilde{\phi}_{ m f} = rac{3}{2} ilde{\phi}_{ m C}$		
Central difference	$\tilde{\phi}_{\mathrm{f}} = \frac{1 - \tilde{\xi}_{\mathrm{f}}}{1 - \tilde{\xi}_{\mathrm{C}}} \tilde{\phi}_{\mathrm{C}} + \frac{\tilde{\xi}_{\mathrm{f}} - \tilde{\xi}_{\mathrm{C}}}{1 - \tilde{\xi}_{\mathrm{C}}}$	$\tilde{\phi}_{\rm f}=0.5~\tilde{\phi}_{\rm C}+0.5$		
FROMM scheme	$\tilde{\phi}_{\rm f} = \tilde{\phi}_{\rm C} + (\tilde{\xi}_{\rm f} - \tilde{\xi}_{\rm C})$	$ ilde{\phi}_{\mathrm{f}} = ilde{\phi}_{\mathrm{C}} + rac{1}{4}$		
QUICK scheme	$\tilde{\phi}_{\rm f} = \frac{\tilde{\xi}_{\rm f}(1-\tilde{\xi}_{\rm f})}{\tilde{\xi}_{\rm C}(1-\tilde{\xi}_{\rm C})}\tilde{\phi}_{\rm C} + \frac{\tilde{\xi}_{\rm f}(\tilde{\xi}_{\rm f}-\tilde{\xi}_{\rm C})}{1-\tilde{\xi}_{\rm C}}$	$\tilde{\phi}_{\rm f} = \frac{3}{4}\tilde{\phi}_{\rm C} + \frac{3}{8}$		

and for $\tilde{\phi}_{\rm C} < 0$ or $\tilde{\phi}_{\rm C} > 1$ the functional relationship $f(\tilde{\phi}_{\rm C})$ should equal $\tilde{\phi}_{\rm C}$. Mathematically, these conditions are

$$CBC = \begin{cases} f(\tilde{\phi}) \text{ is continuous} \\ f(\tilde{\phi}) = 0 \text{ for } \tilde{\phi}_{C} = 0 \\ f(\tilde{\phi}) = 1 \text{ for } \phi_{C} = 1 \\ 1 < f(\tilde{\phi}) < \tilde{\phi}_{C} \text{ for } 0 < \tilde{\phi}_{C} < 1 \\ f(\tilde{\phi}) = \tilde{\phi}_{C} \text{ for } \tilde{\phi}_{C} < 0 \text{ and } \tilde{\phi}_{C} > 1 \end{cases}$$

$$(9)$$

The above conditions may also be described geometrically on a normalized variable diagram (NVD) as shown in Figure 3. In Figure 4, the linear relations given in Table 1 are also plotted on a normalized variable diagram. From this plot, it may easily be seen that the only scheme that fully satisfies the boundedness criterion [Eq. (9)] is the first-order upwind scheme [2]. Therefore, with the exception of this

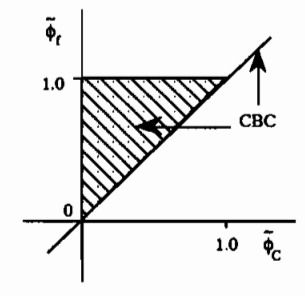


Figure 3. Convective boundedness criterion (CBC).

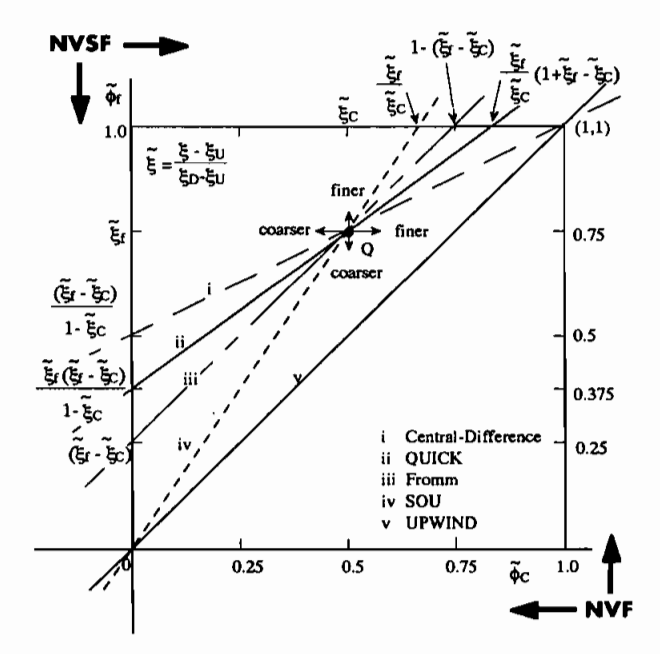


Figure 4. Normalized variable diagram (NVD) for several linear schemes formulated using NVSF.

scheme, other schemes may in general give physically unrealistic results. Furthermore, schemes that have an NVD plot close to the first-order upwind NVD plot tend to be highly diffusive, while schemes whose NVD plots are near the first-order downwind NVD plot (the line $\tilde{\phi}_{\rm f}=1$) tend to be highly compressive.

Normalized Variable and Space Formulation Methodology

Knowing the required conditions for boundedness, the shortcomings of the HO schemes were eliminated through the development of HR schemes that satisfy all above requirements. Without going into details, a number of HR schemes were formulated using the NVSF methodology [8], and the functional relationships for some of them are given in Table 2. The last columns in Tables 1 and 2 show the special uniform-grid form of the functional relationships for the HO and HR schemes obtained by setting $\xi_{\rm C}$ and $\xi_{\rm f}$ to 0.5 and 0.75, respectively. The NVD plots of the composite schemes of Table 2 are shown in Figure 5.

IMPLEMENTATION TECHNIQUES FOR HIGH-RESOLUTION SCHEMES

Having presented the functional relationships of some HR schemes, the DC, DWF, and VCF methods used in implementing them are reviewed, followed by a thorough description of the newly developed NWF method.

Table 2. Functional relationships of a number of high-resolution schemes (composite schemes)

Community	Normalized functional relationships				
Composite schemes	Nonuniform grid (NVSF)	Uniform grid (NVF)			
MINMOD or SOUCOUP	$\tilde{\phi}_{\mathbf{f}} = \begin{cases} \frac{\tilde{\xi}_{\mathbf{f}}}{\tilde{\xi}_{\mathbf{C}}} \tilde{\phi}_{\mathbf{C}} & 0 < \tilde{\phi}_{\mathbf{C}} < \tilde{\xi}_{\mathbf{C}} \\ \frac{1 - \tilde{\xi}_{\mathbf{f}}}{1 - \tilde{\xi}_{\mathbf{C}}} \tilde{\phi}_{\mathbf{C}} + \frac{\tilde{\xi}_{\mathbf{f}} - \tilde{\xi}_{\mathbf{C}}}{1 - \tilde{\xi}_{\mathbf{C}}} & \tilde{\xi}_{\mathbf{C}} < \tilde{\phi}_{\mathbf{C}} < 1 \\ \tilde{\phi}_{\mathbf{C}} & \text{elsewhere} \end{cases}$	$\tilde{\phi}_{f} = \begin{cases} \frac{3}{2}\tilde{\phi}_{C} & 0 < \tilde{\phi}_{C} < \frac{1}{2} \\ \frac{1}{2}\tilde{\phi}_{C} + \frac{1}{2} & \frac{1}{2} < \tilde{\phi}_{C} < 1 \\ \tilde{\phi}_{C} & \text{elsewhere} \end{cases}$			
OSHER	$\tilde{\phi}_{\mathbf{f}} = \begin{cases} \frac{\tilde{\xi}_{\mathbf{f}}}{\tilde{\xi}_{\mathbf{C}}} \tilde{\phi}_{\mathbf{C}} & 0 < \tilde{\phi}_{\mathbf{C}} < \frac{\tilde{\xi}_{\mathbf{C}}}{\tilde{\xi}_{\mathbf{f}}} \\ 1 & \frac{\tilde{\xi}_{\mathbf{C}}}{\tilde{\xi}_{\mathbf{f}}} \leq \tilde{\phi}_{\mathbf{C}} < 1 \\ \tilde{\phi}_{\mathbf{C}} & \text{elsewhere} \end{cases}$	$\tilde{\phi}_{\mathbf{f}} = \begin{cases} \frac{3}{2} \tilde{\phi}_{\mathbf{C}} & 0 < \tilde{\phi}_{\mathbf{C}} < \frac{2}{3} \\ 1 & \frac{2}{3} \leq \tilde{\phi}_{\mathbf{C}} < 1 \\ \tilde{\phi}_{\mathbf{C}} & \text{elsewhere} \end{cases}$			
MUSCL	$\tilde{\phi}_{\mathbf{f}} = \begin{cases} \frac{2\tilde{\xi}_{\mathbf{f}} - \tilde{\xi}_{\mathbf{C}}}{\tilde{\xi}_{\mathbf{C}}} \tilde{\phi}_{\mathbf{C}} & 0 < \tilde{\phi}_{\mathbf{C}} < \frac{\tilde{\xi}_{\mathbf{C}}}{2} \\ \\ \tilde{\phi}_{\mathbf{C}} + (\tilde{\xi}_{\mathbf{f}} - \tilde{\xi}_{\mathbf{C}}) & \frac{\tilde{\xi}_{\mathbf{C}}}{2} < \tilde{\phi}_{\mathbf{C}} < 1 + \tilde{\xi}_{\mathbf{C}} - \tilde{\xi}_{\mathbf{f}} \\ \\ 1 & 1 + \tilde{\xi}_{\mathbf{C}} - \tilde{\xi}_{\mathbf{f}} < \tilde{\phi}_{\mathbf{C}} < 1 \\ \\ \tilde{\phi}_{\mathbf{C}} & \text{elsewhere} \end{cases}$	$\tilde{\phi}_{f} = \begin{cases} 2\tilde{\phi}_{C} & 0 < \tilde{\phi}_{C} < \frac{1}{4} \\ \tilde{\phi}_{C} + \frac{1}{4} & \frac{1}{4} < \tilde{\phi}_{C} < \frac{3}{4} \\ 1 & \frac{3}{4} < \tilde{\phi}_{C} < 1 \\ \tilde{\phi}_{C} & \text{elsewhere} \end{cases}$			
SMART	$\begin{split} \tilde{\phi}_{\mathrm{C}} & \text{elsewhere} \\ & \begin{cases} \frac{\tilde{\xi}_{\mathrm{f}}(1-3\tilde{\xi}_{\mathrm{C}}+2\tilde{\xi}_{\mathrm{f}})}{\tilde{\xi}_{\mathrm{C}}(1-\tilde{\xi}_{\mathrm{C}})} \tilde{\phi}_{\mathrm{C}} & 0 < \tilde{\phi}_{\mathrm{C}} < \frac{\tilde{\xi}_{\mathrm{C}}}{3} \\ \\ \frac{\tilde{\xi}_{\mathrm{f}}(1-\tilde{\xi}_{\mathrm{f}})}{\tilde{\xi}_{\mathrm{C}}(1-\tilde{\xi}_{\mathrm{C}})} \tilde{\phi}_{\mathrm{C}} & \frac{\tilde{\xi}_{\mathrm{C}}}{3} \leq \tilde{\phi}_{\mathrm{C}} < \frac{\tilde{\xi}_{\mathrm{C}}}{\tilde{\xi}_{\mathrm{f}}} \\ \\ \tilde{\phi}_{\mathrm{f}} = \begin{cases} +\frac{\tilde{\xi}_{\mathrm{f}}(\tilde{\xi}_{\mathrm{f}}-\tilde{\xi}_{\mathrm{C}})}{1-\tilde{\xi}_{\mathrm{C}}} & \times (1+\tilde{\xi}_{\mathrm{f}}-\tilde{\xi}_{\mathrm{C}}) \\ \\ 1 & \frac{\tilde{\xi}_{\mathrm{C}}}{\tilde{\xi}_{\mathrm{f}}} (1+\tilde{\xi}_{\mathrm{f}}-\tilde{\xi}_{\mathrm{C}}) \\ \\ \leq \tilde{\phi}_{\mathrm{C}} < 1 \\ \\ \mathrm{elsewhere} \end{cases} \end{split}$	$\tilde{\phi}_{\rm f} = \begin{cases} 3\tilde{\phi}_{\rm C} & 0 < \tilde{\phi}_{\rm C} < \frac{1}{6} \\ \\ \frac{3}{4}\tilde{\phi}_{\rm C} + \frac{3}{8} & \frac{1}{6} \leqslant \tilde{\phi}_{\rm C} < \frac{5}{6} \\ \\ 1 & \frac{5}{6} \leqslant \tilde{\phi}_{\rm C} < 1 \\ \\ \tilde{\phi}_{\rm C} & \text{elsewhere} \end{cases}$			

The Deferred-Correction Method

One way to simplify the implementation of HR schemes is through the use of the DC procedure of Rubin and Khosla [10]. The DC method is a compacting technique that enables the use of HR schemes in codes initially written for LO schemes. Using this procedure, Eq. (2) is rewritten as

$$J_{e}^{LO} + J_{w}^{LO} + J_{n}^{LO} + J_{s}^{LO}$$

$$= B_{P} + \left[C_{e} (\phi_{e}^{LO} - \phi_{e}) + C_{w} (\phi_{w}^{LO} - \phi_{w}) + C_{n} (\phi_{n}^{LO} - \phi_{n}) + C_{s} (\phi_{s}^{LO} - \phi_{s}) \right]$$
(10)

where ϕ_f^{LO} is the face value obtained through the use of a LO scheme, usually the upwind scheme [1], J_f^{LO} is the total flux of ϕ_f^{LO} , ϕ_f is the cell face value calculated using the chosen HR scheme, and the bracketed terms represent the extra source term added due to the DC procedure. Substituting the value of the cell flux obtained from the functional relationship of the LO and HR schemes at hand, the DC technique results in an equation similar in form to Eq. (6), but where the coefficient matrix is pentadiagonal (for two dimensions) and always diagonally dominant, since it is formed using the LO (e.g., upwind) scheme. The discretized equation, Eq. (7), becomes

$$A_{P}\phi_{P} = \sum_{NB} A_{NB}\phi_{NB} + B_{P} + B_{dc}$$
 (11)

where now the coefficients $A_{\rm P}$ and $A_{\rm NB}$ are obtained from a first-order (upwind) discretization, NB=(E, W, N, S) and $B_{\rm dc}$ is the extra deferred-correction source term. This compacting procedure is simple to implement, however, because as the difference between the cell face values calculated with the LO scheme and that calculated with the HR scheme becomes larger, the convergence rate diminishes. This effect can be easily estimated on a NVD; the difference between the upwind line and that of the chosen HR scheme is the normalized difference between the cell face values. The larger this difference is, the lower the convergence rate will be.

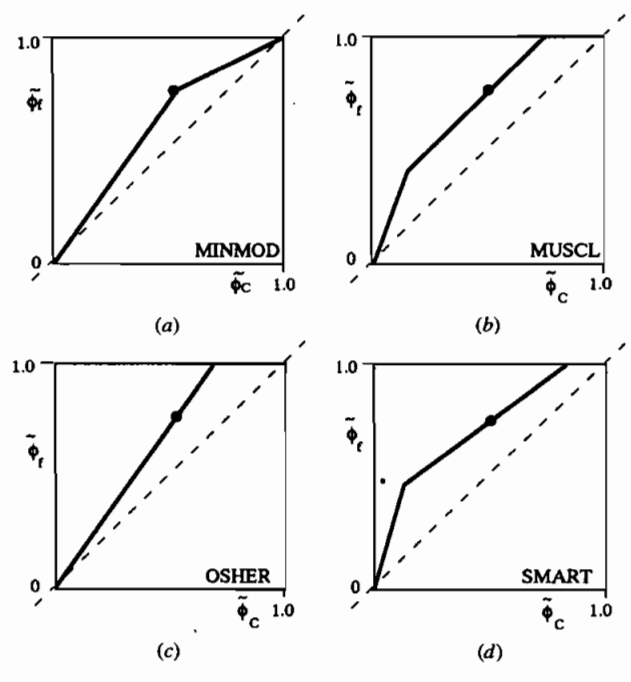


Figure 5. NVD plots for various HR schemes using the NVF and NVSF methodologies.

The Downwind Weighting-Factor Method

The downwind weighting-factor (DWF) method [12] of Leonard generates a compact implicit set of coefficients suitable for tridiagonal solution methods. After explicitly computing the HR scheme estimate of ϕ_f or the normalized value of ϕ_f ($\tilde{\phi}_f$), the DWF is defined as:

$$DWF = \frac{\phi_f - \phi_C}{\phi_D - \phi_C} = \frac{\tilde{\phi}_f - \tilde{\phi}_C}{1 - \phi_C}$$
 (12)

It is clear that the face-value ϕ_f may be written in terms of the known DWF as

$$\phi_{\rm f} = {\rm DWF}\phi_{\rm D} + (1 - {\rm DWF})\phi_{\rm C} \tag{13}$$

where ϕ_D and ϕ_C are to be computed. Thus, by replacing the cell face value of ϕ in Eq. (6) by the above equation, Eq. (6) becomes (for C_e , $C_n > 0$ and C_w , $C_s < 0$)

$$C_{c}[DWF_{c}\phi_{E} + (1 - DWF_{c})\phi_{P}] + C_{w}[DWF_{w}\phi_{P} + (1 - DWF_{w})\phi_{W}]$$

$$+ C_{n}[DWF_{n}\phi_{N} + (1 - DWF_{n})\phi_{P}] + C_{s}[DWF_{s}\phi_{P} + (1 - DWF_{s})\phi_{S}] = B$$
(14)

which can be transformed after some algebraic manipulations into a form similar to Eq. (7):

$$A_{\rm P}\phi_{\rm P} = \sum_{\rm NB = E, W, N, S} A_{\rm NB}\phi_{\rm NB} + B_{\rm P}$$
 (15)

While Eq. (15) has a compact stencil, it was found from experience that the DWF method is highly unstable, and necessitates a very low underrelaxation factor. In order to see clearly the cause of this instability, the one-dimensional form of Eq. (15) is written for a purely convective-flow problem without a source and is given by (for $C_e > 0$ and $C_w < 0$)

$$A_{\rm P}\phi_{\rm P} = A_{\rm E}\phi_{\rm E} + A_{\rm W}\phi_{\rm W} \tag{16}$$

where

$$A_{P} = C_{e}(1 - DWF_{e}) + C_{W}DWF_{w}$$

$$A_{E} = -C_{e}DWF_{e}$$

$$A_{W} = -C_{w}(1 - DWF_{w})$$
(17)

Without loss of generality, assume that $DWF_e = DWF_w = DWF$. Then Eq. (16) shows that A_P becomes negative once the $DWF \ge 0.5$ leading to unphysical results [note that $DWF \ge 0.5$ whenever $\phi_f \ge 0.5(\phi_C + \phi_D)$, which is the case for all HR schemes when $\tilde{\phi}_C > \tilde{\xi}_C$]. This is due to placing large emphasis on the

downwind value as opposite to upwinding. Stated differently, a relation [Eq. (13)] that may not be true is being enforced on ϕ_f . That is, even though ϕ_f is calculated based on the CBC, rewriting it as a weighted average of ϕ_D and ϕ_U via the DWF may cause problems due to its resemblance to the central difference scheme. In addition to the aforementioned problem, the calculation of the DWF based on the evaluation of ϕ_f using the available neighboring ϕ values adds some explicitness to the formulation and slows down the rate of convergence.

The Variable-Curvature-Factor (VCF) Method

The variable-curvature-factor technique was originally developed by Gaskell and Lau [13] and then reformulated by Leonard and Mokhtari [12]. In the context of the NVSF methodology, the equation for the normalized face value is written as

$$\tilde{\phi}_{f} = \left(\frac{1 - \tilde{\xi}_{f}}{1 - \tilde{\xi}_{C}}\tilde{\phi}_{C} + \frac{\tilde{\xi}_{f} - \tilde{\xi}_{C}}{1 - \tilde{\xi}_{C}}\right) - VCF\left(1 - \frac{\tilde{\phi}_{C}}{\tilde{\xi}_{C}}\right)$$
(18)

Rearranging gives

$$VCF = \frac{\left\{ \left[\left(1 - \tilde{\xi}_{f} \right) / \left(1 - \tilde{\xi}_{C} \right) \right] \tilde{\phi}_{C} + \left[\left(\tilde{\xi}_{f} - \tilde{\xi}_{C} \right) / \left(1 - \tilde{\xi}_{C} \right) \right] \right\} - \tilde{\phi}_{f}}{1 - \left(\tilde{\phi}_{C} / \tilde{\xi}_{C} \right)}$$
(19)

For the case of the QUICK scheme, replacing $\tilde{\phi}_f$ by its functional relationship in Eq. (19) gives

$$VCF = \frac{\left(\tilde{\xi}_{f} - \tilde{\xi}_{C}\right)\left(1 - \tilde{\xi}_{f}\right)}{\left(1 - \tilde{\xi}_{C}\right)}$$
(20)

Similar VCF expressions may be obtained for other schemes. For example, VCF = 0 for the second-order differencing scheme, while it is a function of $\tilde{\phi}_{\rm C}$ for the upwind scheme.

Thus, the value of VCF is usually computed from an equation similar to Eq. (20) based on the current value of $\tilde{\phi}_{\rm C}$. Then Eq. (18) is denormalized and written in terms of the "to-be-computed" values as

$$\phi_{f} = \left(\frac{\xi_{D} - \xi_{f}}{\xi_{D} - \xi_{C}}\phi_{C} + \frac{\xi_{f} - \xi_{C}}{\xi_{D} - \xi_{C}}\phi_{D}\right) - VCF\left[\phi_{D} - \phi_{U} - \frac{\xi_{D} - \xi_{U}}{\xi_{C} - \xi_{U}}(\phi_{C} - \phi_{U})\right]$$
(21)

The cell-face values [Eq. (21)] are then substituted in Eq. (6) for the different control-volume faces. After some algebraic manipulation, an equation with a computational stencil involving five points in each direction is obtained as follows:

$$A_{\rm P}\phi_{\rm P} = \sum_{\rm NB=E, W, N, S, EE, WW, NN, SS} A_{\rm NB}\phi_{\rm NB} + B_{\rm P}$$
 (22)

The main problem associated with this method is the need to underrelax the VCF factor to avoid oscillations in the iterative solution process. The reason is that composite schemes for which the NVD plot do not pass through the point (ξ_C , ξ_f) have a VCF that is constantly varying with $\tilde{\phi}_f$. The coefficients of Eq. (22) that depend on the VCF of the cell faces are thus continuously changing, even for small changes in $\tilde{\phi}_f$. This means that important underrelaxation to the VCF factor is needed, leading to a decrease in the convergence rate. Even the upwind scheme, when implemented using this technique, yields an expanded stencil with a relatively low convergence rate.

The New Normalized Weighting-Factor Method

As can be seen, the DC method may result in large source terms that are explicitly calculated, whereas the VCF method requires important underrelaxation to enforce convergence. The DWF method, however, suffers two important drawbacks. First, in calculating the DWF, the value of ϕ_f is used and is calculated from the functional relationship of the HR scheme based on the currently available estimates of the neighboring node values. This introduces some explictness into the formulation. Second, negative A_p coefficients arise whenever the DWF is greater than 0.5. The normalized weighting-factor method is based on the NVSF methodology and is developed keeping the above shortcomings in mind. As can be seen on the NVD diagram, nearly all HR schemes can be written as a set of linear equations of the form

$$\tilde{\phi}_{\rm f} = m\tilde{\phi}_{\rm C} + k \tag{23}$$

where m and k are constants (slope and intercept of the linear function, depending on geometric quantities only) within any interval of $\tilde{\phi}_f$, with the number of the intervals depending on the HR scheme used. For example, by equating Eq. (23) to the NVSF form of the MINMOD scheme, Table 2, the values of m and k are given by:

$$(m,k) = \begin{cases} \left(\frac{\tilde{\xi}_{f}}{\tilde{\xi}_{C}}, 1\right) & 0 < \tilde{\phi}_{C} < \tilde{\xi}_{C} \\ \left(\frac{1 - \tilde{\xi}_{f}}{1 - \tilde{\xi}_{C}}, \frac{\tilde{\xi}_{f} - \tilde{\xi}_{C}}{1 - \tilde{\xi}_{C}}\right) & \tilde{\xi}_{C} \leq \tilde{\phi}_{C} < 1 \\ (1,0) & \text{elsewhere} \end{cases}$$

$$(24)$$

Furthermore, Eq. (23) could also be written as

$$\frac{\phi_{\rm f} - \phi_{\rm U}}{\phi_{\rm D} - \phi_{\rm U}} = m \frac{\phi_{\rm C} - \phi_{\rm U}}{\phi_{\rm U} - \phi_{\rm U}} + k \tag{25}$$

which yields

$$\phi_{\rm f} = m(\phi_{\rm C} - \phi_{\rm H}) + k(\phi_{\rm D} - \phi_{\rm H}) + \phi_{\rm H} = m\phi_{\rm C} + k\phi_{\rm D} + (1 - m - k)\phi_{\rm H}$$
 (26)

where ϕ_U , ϕ_D , and ϕ_C are the upstream, downstream, and central node values of ϕ near the control-volume face at hand. Obviously, these values depend on the flow direction. Defining the following switches,

$$C_f^+ = \max(0, C_f)$$

 $C_f^- = -\max(0, -C_f)$ (27)

and substituting the ϕ_f value for each of the control-volume faces, as given by Eq. (26) into Eq. (6), the following discretized equation is obtained:

$$C_{e}^{+}[m_{e}\phi_{P} + k_{e}\phi_{E} + (1 - m_{e} - k_{e})\phi_{W}]$$

$$+ C_{e}^{-}[m_{e}\phi_{E} + k_{e}\phi_{P} + (1 - m_{e} - k_{e})\phi_{EE}]$$

$$+ C_{w}^{+}[m_{w}\phi_{P} + k_{w}\phi_{W} + (1 - m_{w} - k_{w})\phi_{E}]$$

$$+ C_{w}^{-}[m_{w}\phi_{W} + k_{w}\phi_{P} + (1 - m_{w} - k_{w})\phi_{WW}]$$

$$+ C_{n}^{+}[m_{n}\phi_{P} + k_{n}\phi_{N} + (1 - m_{n} - k_{n})\phi_{S}]$$

$$+ C_{n}^{-}[m_{n}\phi_{N} + k_{n}\phi_{P} + (1 - m_{n} - k_{n})\phi_{NN}]$$

$$+ C_{s}^{+}[m_{s}\phi_{P} + k_{s}\phi_{S} + (1 - m_{s} - k_{s})\phi_{N}]$$

$$+ C_{s}^{-}[m_{s}\phi_{S} + k_{s}\phi_{P} + (1 - m_{s} - k_{s})\phi_{SS}] = B$$
(28)

After some algebraic manipulations, Eq. (28) is written in the form

$$A_{\mathbf{P}}\phi_{\mathbf{P}} = \sum_{\mathbf{NB}=\mathbf{E},\mathbf{W},\mathbf{N},\mathbf{S},\mathbf{EE},\mathbf{WW},\mathbf{NN},\mathbf{SS}} A_{\mathbf{NB}}\phi_{\mathbf{NB}} + B_{\mathbf{P}}$$
 (29)

where the coefficients are given by

$$A_{\rm p} = \left[C_{\rm e}^{+} m_{\rm e} + C_{\rm w}^{+} m_{\rm w} + C_{\rm n}^{+} m_{\rm n} + C_{\rm s}^{+} m_{\rm s} + C_{\rm e}^{-} k_{\rm e} + C_{\rm w}^{-} k_{\rm w} + C_{\rm n}^{-} k_{\rm n} + C_{\rm s}^{-} k_{\rm s} \right]$$

$$A_{\rm E} = -\left[C_{\rm e}^{+} k_{\rm e} + C_{\rm e}^{-} m_{\rm e} + C_{\rm w}^{+} (1 - m_{\rm w} - k_{\rm w}) \right]$$

$$A_{\rm W} = -\left[C_{\rm w}^{+} k_{\rm w} + C_{\rm w}^{-} m_{\rm w} + C_{\rm e}^{+} (1 - m_{\rm e} - k_{\rm e}) \right]$$

$$A_{\rm N} = -\left[C_{\rm n}^{+} k_{\rm n} + C_{\rm n}^{-} m_{\rm n} + C_{\rm s}^{+} (1 - m_{\rm s} - k_{\rm s}) \right]$$

$$A_{\rm S} = -\left[C_{\rm s}^{+} k_{\rm s} + C_{\rm s}^{-} m_{\rm s} + C_{\rm n}^{+} (1 - m_{\rm n} - k_{\rm n}) \right]$$

$$A_{\rm EE} = -C_{\rm e}^{-} (1 - m_{\rm e} - k_{\rm e}) \quad A_{\rm WW} = -C_{\rm w}^{-} (1 - m_{\rm w} - k_{\rm w})$$

$$A_{\rm NN} = -C_{\rm n}^{-} (1 - m_{\rm n} - k_{\rm n}) \quad A_{\rm SS} = -C_{\rm s}^{-} (1 - m_{\rm s} - k_{\rm s})$$

The values of m and k for a number of HO and HR schemes are listed in Table 3 along with their values for the special case of uniform grid.

Table 3. NWF relationships for the schemes of Tables 1 and 2

	Normalized weighting-factor relationships					
Scheme	Nonuniform Grid (NVSF)		Uniform grid (NVF)			
UPWIND SOU	$[m,k] = [1,0]$ $[m,k] = \left[\frac{\tilde{\xi}_t}{\tilde{\xi}_C}, 0\right]$		$[m,k] = [1,0]$ $[m,k] = \left[\frac{3}{2},0\right]$			
Central difference	$[m,k] = \left[\frac{1-\tilde{\xi}_t}{1-\tilde{\xi}_C}, \frac{\tilde{\xi}_t-\tilde{\xi}_C}{1-\tilde{\xi}_C}\right]$		$[m,k] = \left[\frac{1}{2}, \frac{1}{2}\right]$			
FROMM	$[m,k] = [1,\tilde{\xi}_{\rm f} - \tilde{\xi}_{\rm C}]$		$[m,k] = \left[1, \frac{1}{4}\right]$			
QUICK	$[m,k] = \left[\frac{\tilde{\xi}_{\mathfrak{f}}(1-\tilde{\xi}_{\mathfrak{f}})}{\tilde{\xi}_{\mathbb{C}}(1-\tilde{\xi}_{\mathbb{C}})}, \frac{\tilde{\xi}_{\mathfrak{f}}(\tilde{\xi}_{\mathfrak{f}}-\tilde{\xi}_{\mathbb{C}})}{1-\tilde{\xi}_{\mathbb{C}}}\right]$		$[m,k] = \left[\frac{3}{4}, \frac{3}{8}\right]$			
MINMOD or SOUCOUP	$[m,k] = \begin{cases} \left[\frac{\tilde{\xi}_{t}}{\tilde{\xi}_{C}}, 0\right] & 0 < 1 \\ \left[\frac{1 - \tilde{\xi}_{t}}{1 - \tilde{\xi}_{C}}, \frac{\tilde{\xi}_{t} - \tilde{\xi}_{C}}{1 - \tilde{\xi}_{C}}\right] & \tilde{\xi}_{C} \\ [1,0] & \text{else} \end{cases}$: $ ilde{\phi}_{ m C} < ilde{\xi}_{ m C}$ $< ilde{\phi}_{ m C} < 1$ ewhere	$[m,k] = \begin{cases} \left[\frac{3}{2},0\right] \\ \left[\frac{1}{2},\frac{1}{2}\right] \\ [1,0] \end{cases}$	$0 < \tilde{\phi}_{\rm C} < \frac{1}{2}$ $\frac{1}{2} < \tilde{\phi}_{\rm C} < 1$ elsewhere		
OSHER	$[m,k] = \begin{cases} \left[\frac{\tilde{\xi}_{t}}{\tilde{\xi}_{C}}, 0\right] & 0 < \tilde{\phi}_{C} < \frac{\tilde{\xi}_{C}}{\tilde{\xi}_{t}} \\ [0,1] & \frac{\tilde{\xi}_{C}}{\tilde{\xi}_{t}} < \tilde{\phi}_{C} < 1 \\ [1,0] & \text{elsewhere} \end{cases}$		$[m,k] = \begin{cases} \left[\frac{3}{2},0\right] \\ [0,1] \\ [1,0] \end{cases}$	$0 < \tilde{\phi}_{C} < \frac{2}{3}$ $\frac{2}{3} < \tilde{\phi}_{C} < 1$ elsewhere		
MUSCL	$\{m,k\} = \begin{cases} \left[\frac{2\bar{\xi}_{1} - \bar{\xi}_{C}}{\bar{\xi}_{C}}, 0\right] & 0 < \tilde{\phi}_{C} \\ \left[1, \bar{\xi}_{1} - \bar{\xi}_{C}\right] & \frac{\bar{\xi}_{C}}{2} < \tilde{\phi}_{C} \\ + \tilde{\xi}_{C} \\ \left[0, 1\right] & 1 + \bar{\xi}_{C} - \\ \left[1, 0\right] & \text{elsewher} \end{cases}$	$<\frac{\tilde{\xi}_{C}}{2}$ $C < 1$ $C - \tilde{\xi}_{I}$ $-\tilde{\xi}_{I} < \tilde{\phi}_{C} < 1$ The	$[m,k] = \begin{cases} [2,0] \\ [1,\frac{1}{4}] \\ [0,1] \\ [1,0] \end{cases}$	$0 < \tilde{\phi}_{C} < \frac{1}{4}$ $\frac{1}{4} < \tilde{\phi}_{C} < \frac{3}{4}$ $\frac{3}{4} < \tilde{\phi}_{C} < 1$ elsewhere		
SMART	$[m,k] = \begin{cases} [0,1] & 1 + \tilde{\xi}_{C} - \\ (1,0] & \text{elsewher} \end{cases}$ $\begin{cases} \left[\frac{\tilde{\xi}_{f}(1 - 3\tilde{\xi}_{C} + 2\tilde{\xi}_{f})}{\tilde{\xi}_{C}(1 - \tilde{\xi}_{C})}, 0 \right] \\ \left[\frac{\tilde{\xi}_{f}(1 - \tilde{\xi}_{f})}{\tilde{\xi}_{C}(1 - \tilde{\xi}_{C})}, \frac{\tilde{\xi}_{f}(\tilde{\xi}_{f} - \tilde{\xi}_{C})}{1 - \tilde{\xi}_{C}} \right] \\ [0,1] \\ [1,0] \end{cases}$	$0 < \tilde{\phi}_{C} < \frac{\tilde{\xi}_{C}}{3}$ $\frac{\tilde{\xi}_{C}}{3} < \tilde{\phi}_{C} < \frac{\tilde{\xi}_{C}}{\tilde{\xi}_{f}}$ $\times (1 + \tilde{\xi}_{f} - \tilde{\xi}_{C})$ $\frac{\tilde{\xi}_{C}}{\tilde{\xi}_{f}} (1 + \tilde{\xi}_{f} - \tilde{\xi}_{C})$ $< \tilde{\phi}_{C} < 1$ elsewhere	$[m,k] = \begin{cases} [4,0] \\ \left[\frac{3}{4}, \frac{3}{8}\right] \\ [0,1] \\ [1,0] \end{cases}$	$0 < \tilde{\phi}_{C} < \frac{1}{6}$ $\frac{1}{6} \le \tilde{\phi}_{C} < \frac{5}{6}$ $\frac{5}{6} \le \tilde{\phi}_{C} < 1$ elsewhere		

As can be seen, the resulting discretized equation [Eq. (29)] has a computational stencil involving five grid points in each coordinate direction, which is solved here by applying iteratively the pentadiagonal matrix algorithm (PDMA) in each coordinate direction.

Since for all HR schemes the value of m is greater than that of k (Figure 5), except in a narrow region of the NVD close to the downwind line as explained next, the value of A_P is always positive and instability does not arise. Along the downwind line of the NVD, where (m, k) = (0, 1), a value of zero for the A_P coefficient is obtained. In this case (m, k) is set to $(M, 1 - M\tilde{\phi}_f)$, where M is usually set to the value of m in the previous interval in the composite scheme.

It is also worth mentioning that the NWF method can be combined with the deferred-correction technique when using the Super-C scheme of Leonard [19]. In this case the value of $B_{\rm dc}$ is less important than it would be if the combination was between the hybrid and fifth-order scheme, and hence higher URF can be used.

To elaborate further, in contrast to the DWF and VCF techniques, the new NWF method is fully implicit, except in a narrow region close to the downwind line, and numerically stable since it guarantees positive $A_{\rm P}$ coefficients. The test problems presented next show the effectiveness, high rate of convergence, and virtues of this approach.

TESTS AND RESULTS

The performance of the various HO and HR convective schemes implemented using both the DC and NWF methods is examined in this section by solving two test problems. Results were obtained by covering the physical domain with a 20×20 highly nonuniform grid. In addition, calculations were also performed for the special case of a uniform grid. This was intended to check whether the performance of the method is independent of the grid used. In both tests, computational results were considered converged when the residual error (RE), defined as

$$RE = \sum \left| A_{P} \phi_{P} - \left(\sum_{NB=E,W,N,S,EE,WW,NN,SS} A_{NB} \phi_{NB} + B_{P} + qB_{dc} \right) \right|$$
 (31)

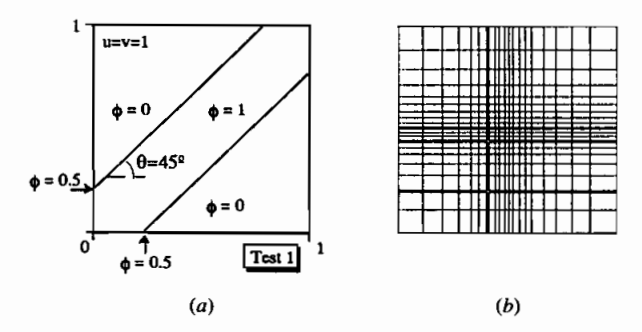


Figure 6. (a) Pure convection of a double-step scalar discontinuity. (b) Nonuniform grid used for the NVSF solution.

where q = 1 for the DC approach and q = 0 for the NWF method, became smaller than 0.001.

Pure Convection of a Double-Step Profile

Figure 6a shows the first benchmark test problem, consisting of a pure convection of a transverse double-step profile imposed at the inflow boundaries of a square computational domain. The nonuniform grid network used in conjunction

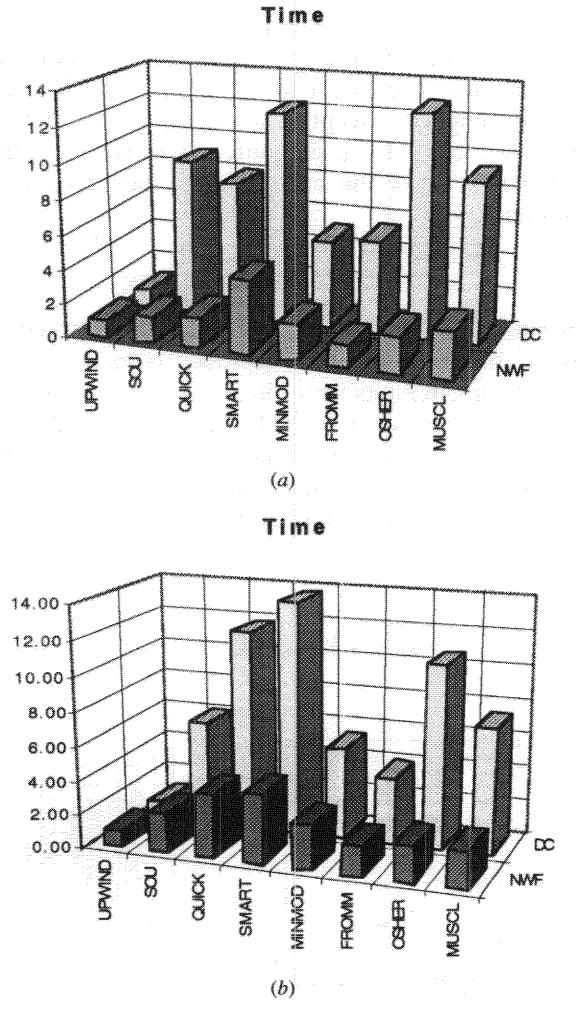


Figure 7. Time comparison for test 1: (a) uniform grid; (b) nonuniform grid.

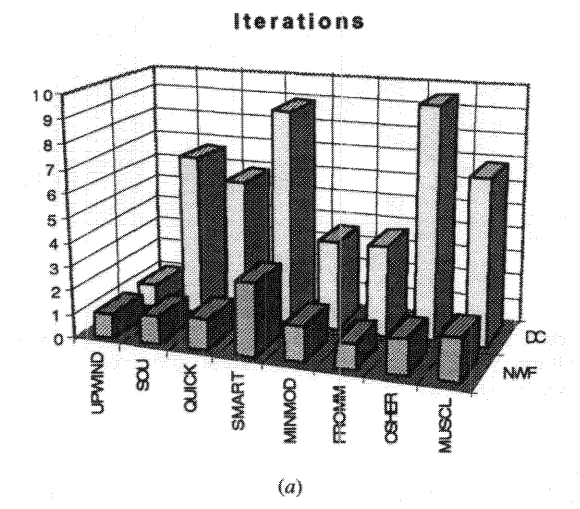


Figure 8. Comparison of number of iterations for test 1: (a) uniform grid; (b) nonuniform grid.

with the NVSF methodology is depicted in Figure 6b. The governing conservation equation of the problem is

$$\frac{\partial(\rho u\phi)}{\partial x} + \frac{\partial(\rho v\phi)}{\partial y} = 0 \tag{32}$$

where ϕ is the dependent variable and u and v are the Cartesian components of the uniform velocity \mathbf{v} , which, in this problem is taken to be at an angle of 45° with respect to the horizontal and of magnitude equal to 1.414. It should be mentioned

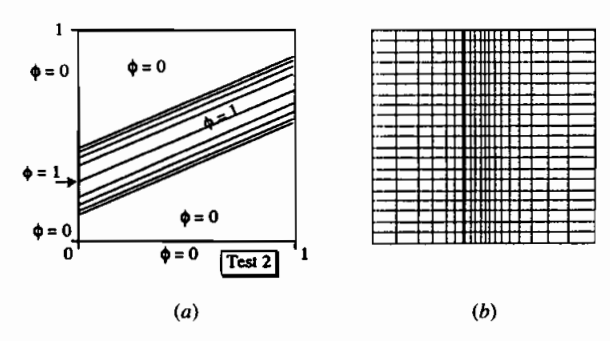


Figure 9. (a) Pure convection of an elliptic profile by a uniform velocity field. (b) Nonuniform grid used for the NVSF solution.

here that converged results obtained with HO schemes showed over- and undershoots.

Comparisons of the computational time and iterations obtained for the NVF and NVSF solutions of the problem using the various HO, HR, and upwind schemes are shown in Figures 7 and 8. The data was normalized with respect to the values obtained from the upwind scheme for which a value of 1 was set. It can be seen very clearly that important economies in computational cost (Figures 7a and 7b) and number of iterations (Figures 8a and 8b) are achieved by using the NWF technique with uniform and nonuniform meshes. This is due to the implicitness and numerical stability of the technique, which always results in a diagnonally dominant system of equations. Further, it was possible with the NWF, and for all schemes, to obtain converged solutions with an underrelaxation factor of 0.9. For the DC procedure, however, the optimum underrelaxation factor was not greater than 0.45 for some of the schemes.

Quantitatively, Figures 7 and 8 show, on average, the NWF method to be four times as fast as the DC method. Furthermore, the distribution of the grid does not affect the performance of the method (compare Figures 7a and 7b and Figures 8a and 8b).

Convection of an Elliptic Profile in an Oblique Velocity Field

This second problem, illustrated in Figure 9a, was used in order to test the acceleration rate of the NWF method for a profile involving a gradually decreasing gradient. The nonuniform grid employed is displayed in Figure 9b. The governing equation of the problem is the same as for test 1 [Eq. (32)]. The elliptic profile is generated using the following equation:

$$\phi = \sqrt{1 - \frac{(j-7)^2}{6^2}} \qquad \text{for } 2 \le j \le 12$$
 (33)

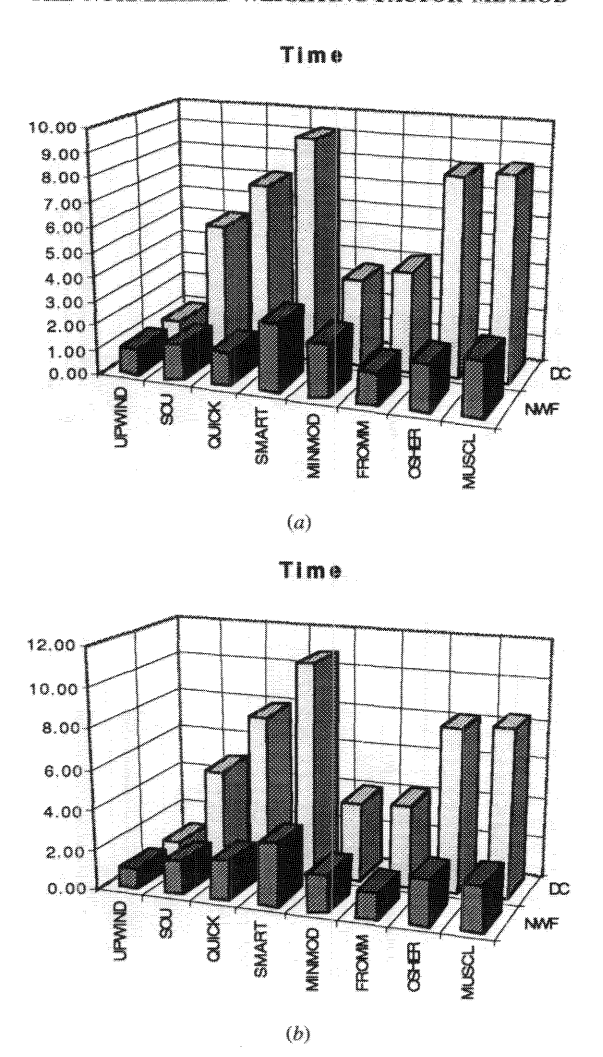
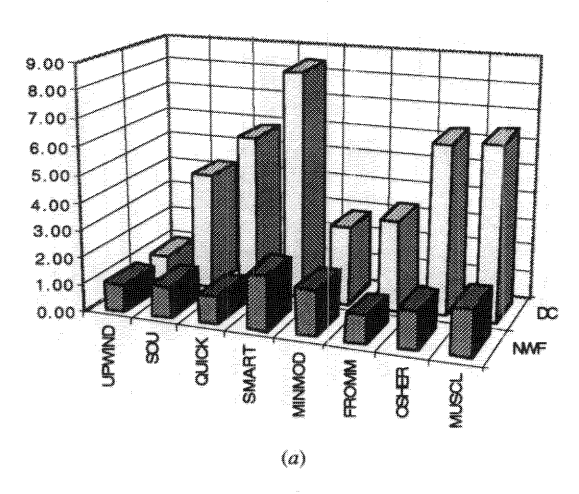


Figure 10. Time comparison for test 2: (a) uniform grid; (b) nonuniform grid.

The normalized time and number of iterations needed to solve the problem on uniform and nonuniform meshes using the various schemes are depicted in Figures 10 and 11, respectively. The trend of results is similar to that of test 1, with a slight increase or decrease in the acceleration rate depending on the scheme. In all cases, however, the NWF method is much faster than the DC method (for uniform and nonuniform grids), with the average acceleration rate being around 4 to 1. This once more shows the superiority of the new NWF method over the DC technique.

Iterations



Iterations

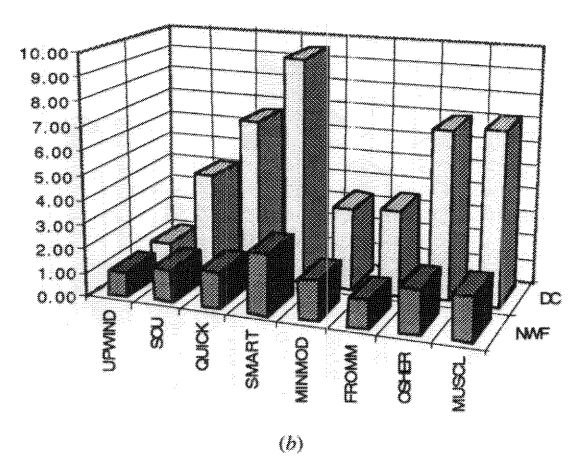


Figure 11. Comparison of number of iterations for test 2: (a) uniform grid; (b) nonuniform grid.

CONCLUDING REMARKS

A new NWF method for accelerating the rate of convergence of convective flow problems discretized using HR schemes was presented. The approach is fully implicit and is applicable to the classes of NVSF and TVD schemes. The numerical implementation of the technique resulted in a discretized equation with a computational stencil of five points in each coordinate direction, which was solved using the PDMA. The method was compared qualitatively with the DWF and VCF methods and was shown to be superior. Quantitative assessment of the new technique against the DC procedure was performed by solving for two test problems. An average acceleration rate of 4 to 1 was obtained. With such a decrease in

computational cost, the NWF method may become a serious competitor to the upwind class of schemes, and will eventually decrease their undeserved popularity.

REFERENCES

- D. B. Spalding, A Novel Finite-Difference Formulation for Differential Expressions Involving Both First and Second Derivatives, Int. J. Numer. Meth. Eng., vol. 4, pp. 551-559, 1972.
- 2. S. V. Patankar, Numerical Heat Transfer and Fluid Flow, Hemisphere, New York, 1981.
- S. A. Syed, L. M. Chiapetta, and A. D. Gosman, Error Reduction Program: Final Report, NASA Contractor Report NASA-CR-174776, 1985.
- 4. W. Shyy, A Study of Finite Difference Approximations to Steady State Convection Dominated Flows, J. Comput. Phys., vol. 57, pp. 415-438, 1985.
- B. P. Leonard, A Stable and Accurate Convective Modelling Procedure Based on Quadratic Interpolation, Comput. Meth. Appl. Mech. Eng., vol. 19, pp. 59-98, 1979.
- B. P. Leonard, Simple High Accuracy Resolution Program for Convective Modeling of Discontinuities, Int. J. Numer. Meth. Eng., vol. 8, pp. 1291-1319, 1988.
- M. S. Darwish, A Comparison of Six High Resolution Schemes Formulated Using the NVF Methodology, 33rd Science Week, Alleppo, Syria, 1993.
- M. S. Darwish and F. Moukalled, Normalized Variable and Space Formulation Methodology for High-Resolution Schemes, *Numer. Heat Transfer*, *Part B*, vol. 26, pp. 79-96, 1994.
- P. K. Sweeby, High Resolution Schemes Using Flux-Limiters for Hyperbolic Conservation Laws, SIAM J. Numer. Anal., vol. 21, pp. 995-1011, 1984.
- S. G. Rubin and P. K. Khosla, Polynominal Interpolation Method for Viscous Flow Calculations, J. Comput. Phys., vol. 27, pp. 153-168, 1982.
- B. P. Leonard and J. E. Drummond, Why You Should Not Use "Hybrid," "Power-Law" or Related Exponential Schemes for Convective Modelling—There Are Much Better Alternatives, *Int. J. Numer. Meth. Fluids*, vol. 20, pp. 421-442, 1995.
- B. P. Leonard and S. Mokhtari, Beyond First-Order Upwinding: The Ultra-Sharp Alternative for Non-Oscillatory Steady-State Simulation of Convection, *Int. J. Numer. Meth. Eng.*, vol. 30, pp. 729-766, 1990.
- P. H. Gaskell and A. K. C. Lau, Curvature Compensated Convective Transport: SMART, a New Boundedness Preserving Transport Algorithm, *Int. J. Numer Meth. Fluids*, vol. 8, pp. 617–641, 1988.
- A. Harten, High Resolution Schemes for Hyperbolic Conservation Laws, J. Comput. Phys., vol. 49, no. 3, pp. 357-393, 1983.
- S. R. Chakravarthy and S. Osher, High Resolution Applications of the OSHER Upwind Scheme for the Euler Equations, AIAA Paper 83-1943, 1983.
- B. Van Leer, Towards the Ultimate Conservative Difference Scheme. V. A Second-Order Sequel to Godunov's Method, J. Comput. Phys., vol. 23, pp. 101–136, 1977.
- J. E. Fromm, A Method for Reducing Dispersion in Convective Difference Schemes, J. Comput. Phys., vol. 3, pp. 176-189, 1968.
- B. P. Leonard, The EULER-QUICK Code, in C. Taylor, J. A. Johnson, and W. R. Smith (eds.), Numerical Methods in Laminar and Turbulent Flow, Pineridge Press, Swansea, UK, pp. 489–499, 1983.
- B. P Leonard, The ULTIMATE Conservative Difference Scheme Applied to Unsteady One-Dimensional Advection, Comput. Meth. Appl. Mech. Eng., vol. 88, pp. 17-74, 1991.